Precision measurements of jets and photons in ATLAS

XII International Conference on New Frontiers in Physics
OAC, Kolymbari, Crete, Greece

Miguel Villaplana
IFIC (University of Valencia and CSIC)

on behalf of the ATLAS Collaboration

July 17th, 2023

IFIC INSTITUT DE FÍSICA CORPUSCULAR · VNIVERSITAT DE VALÈNCIA · CSIC CONSEJO SUPERIOR DE INVESTIGACIONES CIENTÍFICAS · Gen-T · GENERALITAT VALENCIANA

Outlook

- **Measurements of inclusive isolated-photon cross sections provide**
  - a testing ground for pQCD with a hard colourless probe
  - constraints on the proton PDFs
  - input to understand QCD background to Higgs production and BSM searches
- **Event shapes** are a class of observables defined as functions of the final-state particles four-momenta, which **characterise the hadronic energy flow in a collision**
  - The study of these observables in multijet production provides stringent tests of pQCD

- **Focus on three measurements in this talk:**
  - Inclusive-photon production and its dependence on photon isolation [arXiv.2302.00510]
  - Determination of the strong coupling constant from transverse energy-energy correlations in multijet events [arXiv.2301.09351]
  - Measurements of multijet event isotropies using optimal transport [arXiv.2305.16930]

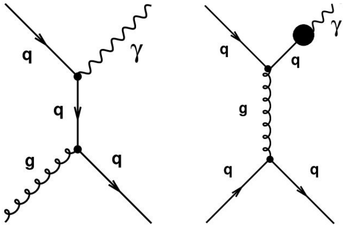

(a) (b)

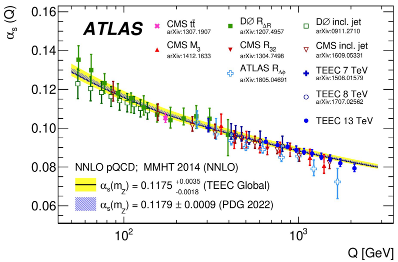

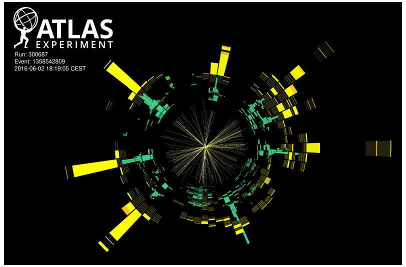

A complete list of ATLAS Standard Model results can be found here: https://twiki.cern.ch/twiki/bin/view/AtlasPublic/StandardModelPublicResults

Prompt photons in pp collisions

- Prompt photons in pp collisions are produced via two mechanisms:

Direct-photon

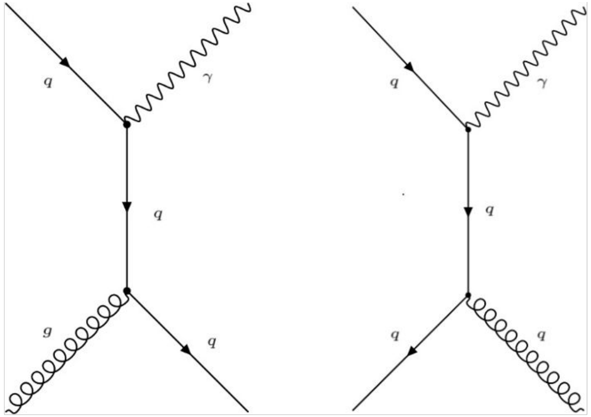

Fragmentation processes

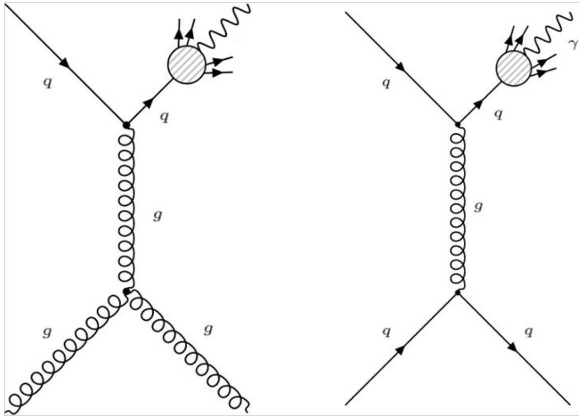

Prompt photon in pp collisions

- In addition to prompt photons, photons are produced copiously inside jets (eg, π^0 decays)
  - it is essential to require isolation to study prompt photons in hadron colliders

- The isolation requirement is based on the energy deposited inside a circle of radius R centered on the photon in the η–ϕ plane (not counting energy depositions coming from the photon itself)

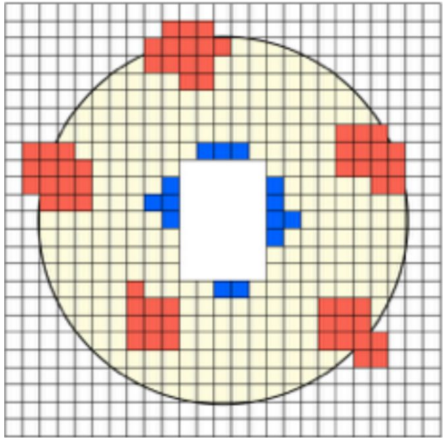

$$E_{\mathrm{T}}^{\mathrm{iso}} \equiv \sum_i E_T^i < E_T^{\mathrm{max}}$$

➪ It is able to suppress most of the contribution of photons inside jets (from π^0's and other neutral mesons decays) and the fragmentation contribution

Inclusive photon production: overview

arXiv.2302.00510

- **Full Run-2 analysis of inclusive-isolated photon cross sections**
- Diferential cross sections measured for two photon isolation cone sizes: R=0.2 and R=0.4
- Test the R-dependence of the inclusive photon cross sections at 13 TeV. [**motivation:** JHEP 04 (2020) 166]
- Fine $|\eta^\gamma|$ binning: [0.0, 0.6, 0.8, 1.37, 1.56, 1.81, 2.01, 2.37]
  - Detailed experimental information for PDF fits

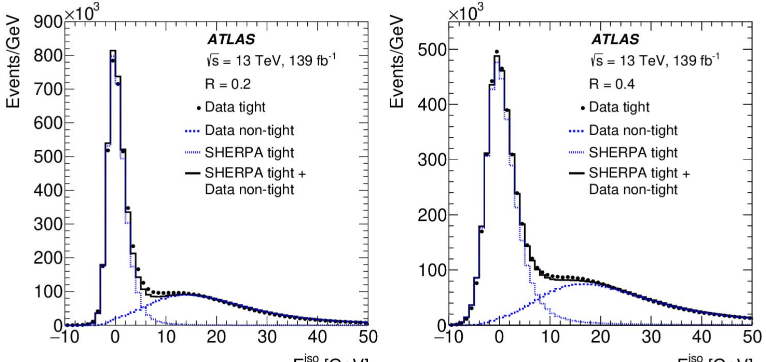

(a) (b)

- Photon selection:
  - $E_T^\gamma > 250$ GeV and $|\eta^\gamma| < 2.37$, excluding the region $1.37 < |\eta^\gamma| < 1.56$
  - photon ID
  - photon isolation: $E_T^{iso} < 4.8\ \text{GeV} + 4.2\cdot10^{-3} \times E_T^\gamma$

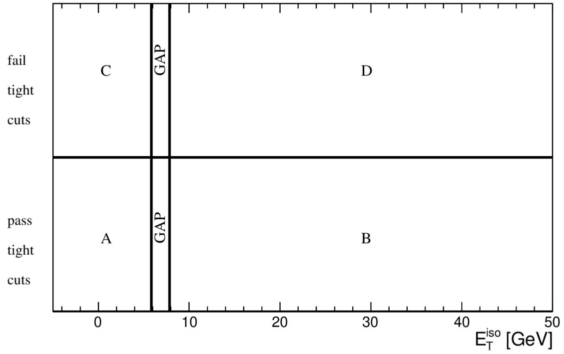

- Background subtracted with data-driven technique
  - control region created by inverting part of the photon ID and isolation requirements.

Inclusive photon production: theoretical predictions

arXiv.2302.00510

JETPHOX (fixed order)

- **Full fixed-order NLO pQCD calculations for direct and fragmentation processes**
- **Scales:** $\mu_R = \mu_F = \mu_f = E_T^{\gamma}/2\,(E_T^{\gamma})$
- **Fragmentation functions:** BFG II
- **PDFs:** MMHT2014, CT18, NNPDF3.1, and HERAPDF2.0 at NLO; ATLASpdf21 at NNLO
- **Isolation:** fixed cone at parton level
- **Non-perturbative corrections:** estimated using PYTHIA samples. Consistent with unity within $\pm 1\,\%$ (no correction applied)

SHERPA NLO (multileg merged)

- **Parton-level calculations for $\gamma + 1{,}2\,(3{,}4)$ jets at NLO (LO) supplemented with PS**
- Only direct contribution (Frixione's isolation at ME level)
- **Scales:** dynamic scale setting (E_T^{γ})
- **PDFs:** NNPDF3.0 NNLO
- **Fragmentation into hadrons and UE simulated as for SHERPA LO**
- **Isolation:** fixed cone at particle level

NNLOJET (fixed order)

- **Full fixed-order NNLO pQCD calculations for direct and fragmentation processes**
- **Scales:** $\mu_R = \mu_F = E_T^{\gamma}$

$$\mu_f = \sqrt{E_T^{\gamma} \cdot E_T^{\max}} \cdot R$$

- **Fragmentation functions:** BFG II
- **PDFs:** CT18 NNLO
- **Isolation:** fixed cone at parton level
- **Non-perturbative corrections:** same estimation as for JETPHOX

- **Theoretical uncertainties:** scale variations (scales x 0,5 or x 2 varied singly or simultaneously), PDFs, α_s, and non-perturbative corrections (only for JETPHOX & NNLOJET)
- NNLO scale uncertainties reduced by more than a factor 2 compared to those of NLO JETPHOX and SHERPA calculations

Inclusive photon production: differential cross sections

arXiv.2302.00510

- Measured cross sections compared to the NLO QCD predictions of JETPHOX as a function of E_T^{γ} in the different $|\eta^{\gamma}|$ regions
  - **Several PDFs compared:** MMHT2014, CT18, NNPDF3.1, HERAPDF2.0, and ATLASpdf21

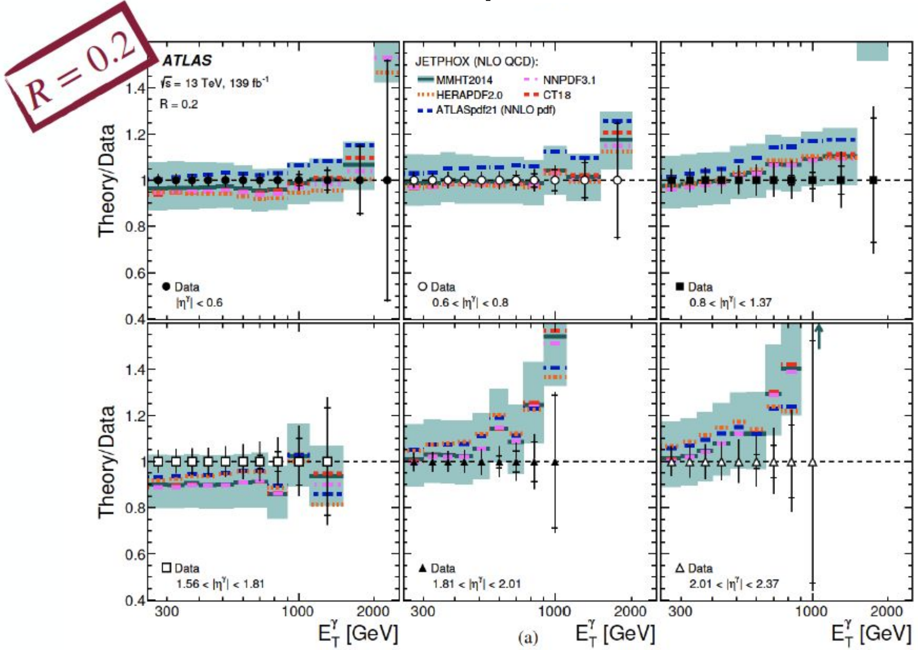

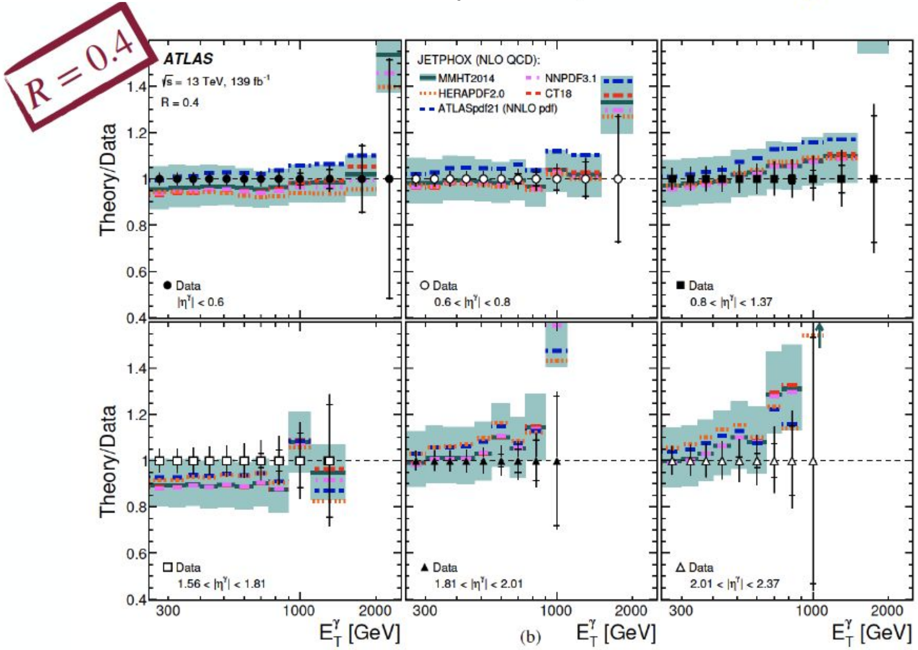

- **Systematic uncertainties** dominated by the photon energy scale, luminosity, pile-up and correlation R^{bg}.
  - Total uncertainty in the range 3% - 20%, depending on the E_T^{γ} and $|\eta^{\gamma}|$ region.

Inclusive photon production: ratios of differential cross sections

arXiv.2302.00510

- The dependence on of the cross sections is studied by measuring the ratios of the differential cross sections for R=0.2 and R=0.4 as functions of E_T^γ in the different $|\eta^\gamma|$ regions

- These measurements provide a **very stringent test of pQCD with reduced experimental and theoretical uncertainties (both ~1% !)**
  - Validation of the underlying pQCD theoretical description up to $\mathcal{O}(\alpha_s^2)$

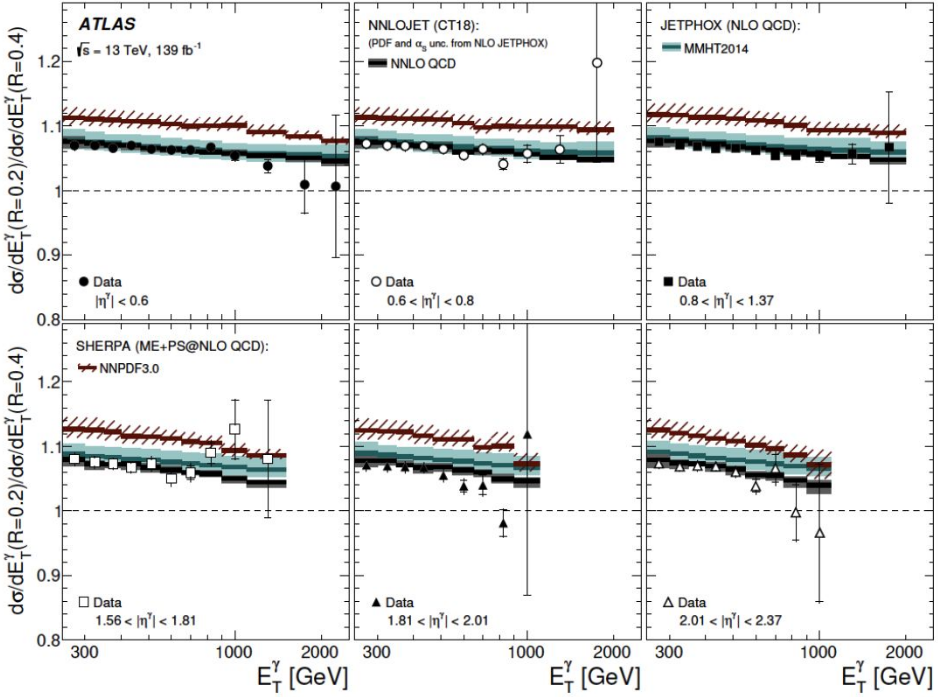

Transverse energy-energy correlations: overview

arXiv.2301.09351

- **TEEC function:** transverse energy-weighted distribution of the azimuthal differences between jet pairs in the final state

$$\frac{1}{\sigma}\frac{d\Sigma}{d\cos\phi} = \frac{1}{N}\sum_{A=1}^{N}\sum_{ij}\frac{E_{Ti}^{A}E_{Tj}^{A}}{\left(\sum_k E_{Tk}^{A}\right)^2}\delta\left(\cos\phi - \cos\varphi_{ij}\right)$$

  - Event shape used in e^+e^-, adapted to pp
  - Essentially an energy-weighted ratio of three-jet to two-jet cross-sections

- **ATEEC function:** difference between the forward ($\cos\Phi > 0$) and backward ($\cos\Phi < 0$) parts of the TEEC function
  - Large sensitivity to QCD radiation and the strong coupling constant
  - Mild sensitivity to PDFs and factorisation and renormalisation scale variations

- **Full Run-2 analysis performed using 139 fb^{-1}**

- Analysis strategy:
  - at least 2 jets with $p_T > 60$ GeV, $|y^{jet}| < 2.4$
  - $H_{T2} = p_{T1} + p_{T2} > 1$ TeV

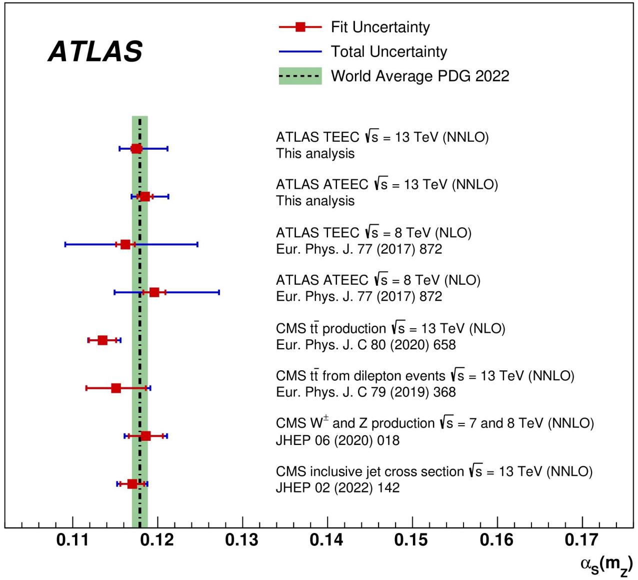

Transverse energy-energy correlations: measured observables

arXiv.2301.09351

- Measured cross section compared to the MC predictions of PYTHIA, SHERPA and HERWIG, for the TEEC (left) and ATEEC (right) distributions in the inclusive H_{T2} bin

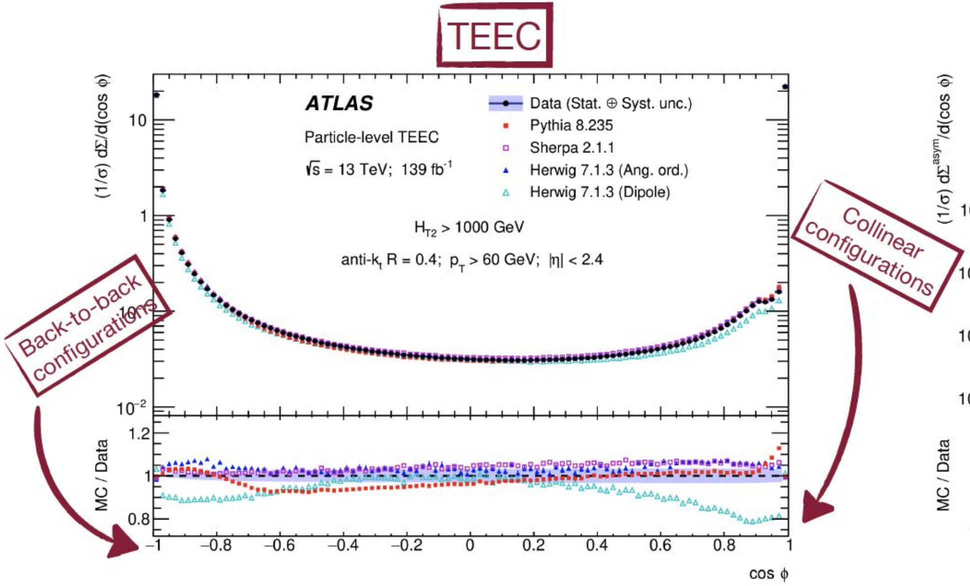

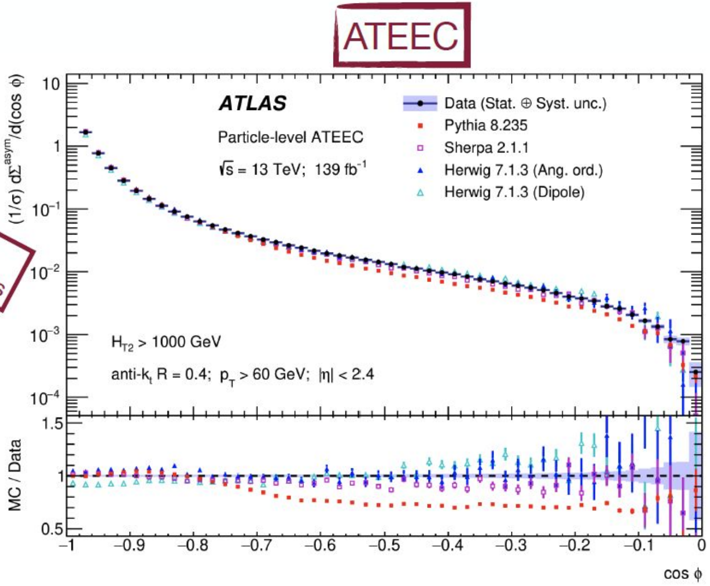

- **Systematic uncertainties** dominated by the jet energy scale and the Monte Carlo model used to correct for detector effects. Total uncertainty of order 2%(1%) for the TEEC (ATEEC).

Transverse energy-energy correlations: theoretical predictions

arXiv.2301.09351

- Full fixed-order NNLO theoretical predictions for 3-jet cross sections obtained by M. Czakon, A. Mitov and R. Poncelet [Phys. Rev. Lett. 127 (2021) 152001, arXiv:2301.01086]

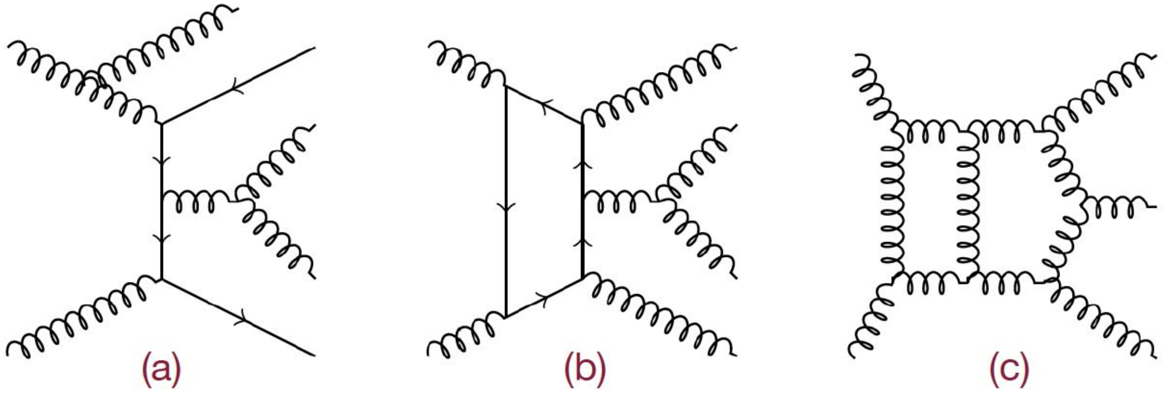

- NNLO corrections calculated using $\mathcal{O}(10^{13})$ events, including real-real (a), virtual-real (b), and virtual-virtual (c) finite terms
  - Renormalisation and factorisation scales fixed to the scalar sum of all final-state partons
  - Non-perturbative corrections estimated using PYTHIA, close to unity within 0.5% for most of the phase space
  - **Theoretical uncertainties:** scale variations, PDFs and non-perturbative corrections uncertainties
    - Reduction by a factor 3 in the cross sections for both TEEC and ATEEC and in the determination of α_s

Transverse energy-energy correlations: results

arXiv.2301.09351

TEEC

$H_{T2} = p_{T1} + p_{T2}$

ATEEC

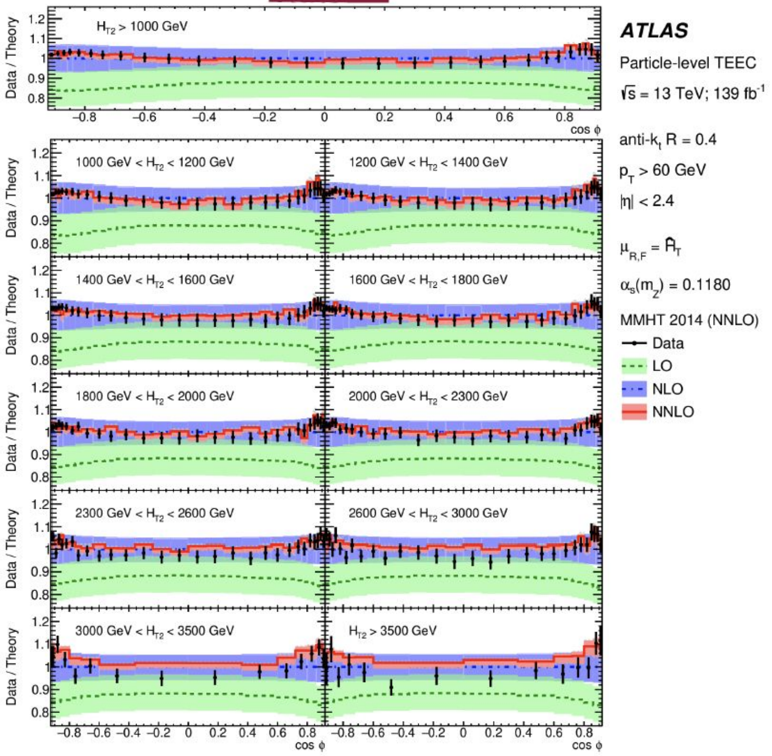

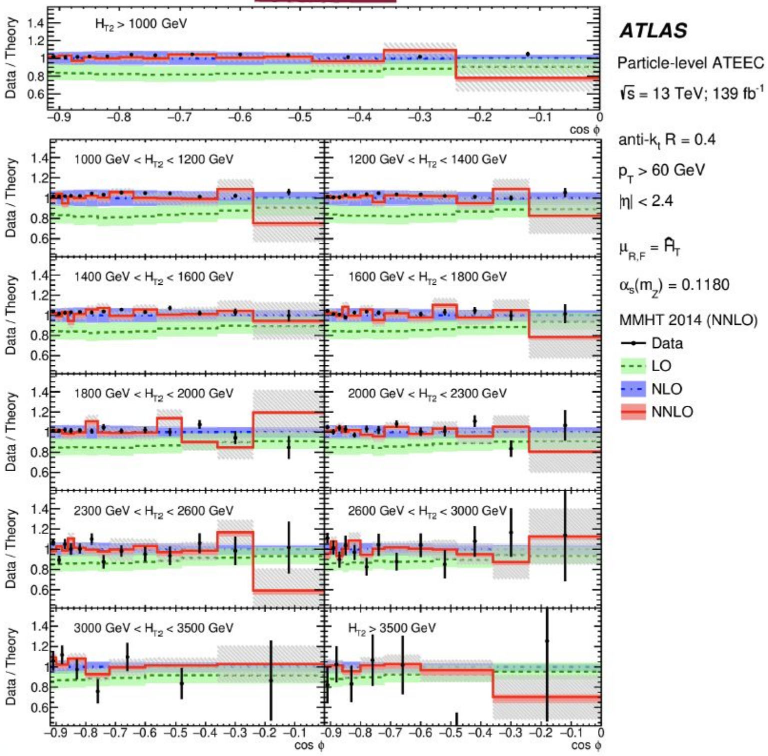

- Excellent agreement between the data and theory with reduced theoretical uncertainties

Transverse energy-energy correlations: determination of $\alpha_s(Q)$

arXiv.2301.09351

- Determination of $\alpha_s(Q)$ from the TEEC in 10 intervals at NNLO accuracy in pQCD, probing asymptotic freedom beyond the TeV scale

- Values of $\alpha_s(m_Z)$ obtained for both the inclusive and 10 exclusive bins in H_{T2} using a χ^2 fit

- The evolution of the $\alpha_s(m_Z)$ values from each of the exclusive fits leads to $\alpha_s(Q)$ values that are compared with the NNLO solution of the RGE

- Global fit results:

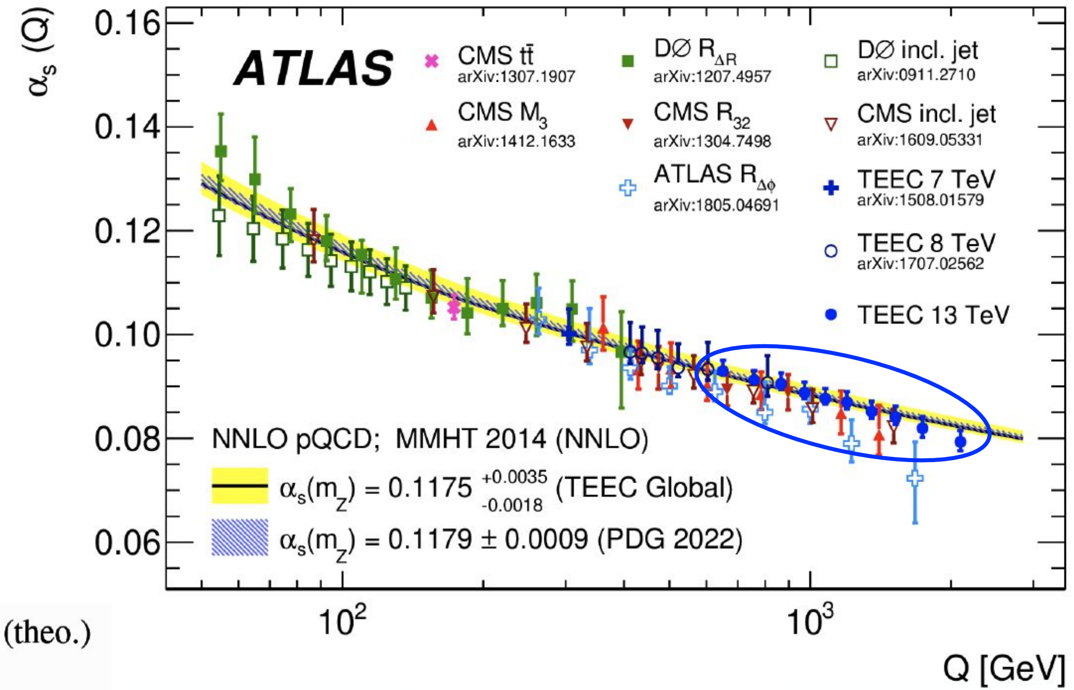

TEEC: $\alpha_s(m_Z) = 0.1175 \pm 0.0006\,(\text{exp.})^{+0.0034}_{-0.0017}\,(\text{theo.})$

ATEEC: $\alpha_s(m_Z) = 0.1185 \pm 0.0009\,(\text{exp.})^{+0.0025}_{-0.0012}\,(\text{theo.})$

Event isotropies using optimal transport: the Energy-Mover's distance

arXiv.2305.16930

- **Event isotropies** quantify how "far" a collider event $\mathcal{E}$ is from a symmetric radiation pattern $\mathscr{U}$, in terms of a Wasserstein distance metric

- **The Energy-Mover's Distance (EMD)** is defined as the minimum amount of "work" needed to transport one event $\mathcal{E}$ into another $\mathcal{E}'$ of equal energy, by a transportation plan f_{ij}, from particle i in one event, to particle j in another

$$\mathrm{EMD}_\beta(\mathscr{E}, \mathscr{E}') = \min_{\{f_{ij}\geq 0\}} \sum_{i=1}^{M} \sum_{j=1}^{M'} f_{ij}\, \theta_{ij}^{\beta},$$

θ_{ij}^{β}: ground measure between particles

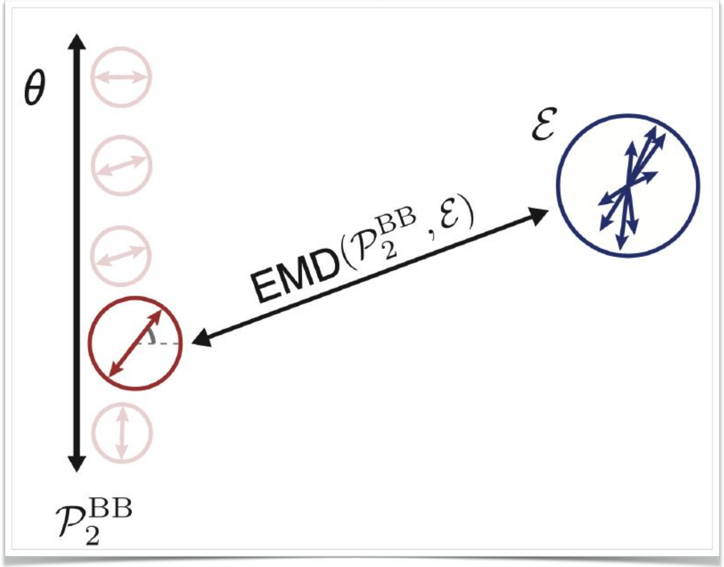

- This EMD uses a Wasserstein metric evaluated by solving the **Optimal Transport** problem

- The event isotropies are defined as $I(\mathcal{E}) = \mathrm{EMD}(\mathcal{E}, \mathscr{U})$ bounded on $I(\mathcal{E}) \in [0,1]$ and infrared- and collinear-safe by construction

Event isotropies using optimal transport: observables

arXiv.2305.16930

- **Three event shape observables are considered in this analysis:**

Geometry	Energy weight	Ground measure	Radiation pattern
Cylinder	$w_i^{\text{Cyl}} = p_{\text{T}i}/p_{\text{T tot}}$	$\theta_{ij}^2 = \frac{12}{\pi^2 + 16y_{\text{max}}^2}(y_{ij}^2 + \phi_{ij}^2)$	$\mathcal{U}_{16}^{\text{Cyl}}$
Ring	$w_i^{\text{Ring}} = p_{\text{T}i}/p_{\text{T tot}}$	$\theta_{ij}^2 = \frac{\pi}{\pi - 2}(1 - \cos\phi_{ij})$	$\mathcal{U}_{128}^{\text{Ring}}$
Ring (dipole)	$w_i^{\text{Ring}} = p_{\text{T}i}/p_{\text{T tot}}$	$\theta_{ij}^2 = \frac{1}{1 - 1/\sqrt{3}}(1 - \cos\phi_{ij})$	$\mathcal{U}_{2}^{\text{Ring}}$

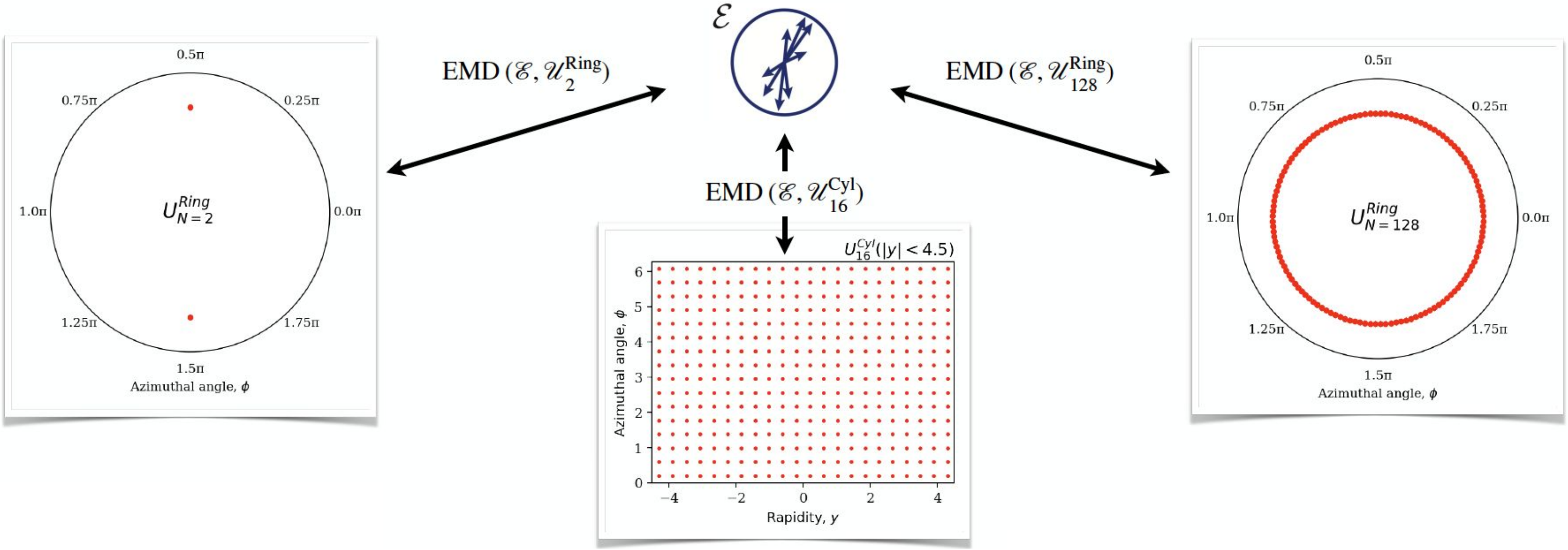

Event isotropies using optimal transport: analysis strategy

arXiv.2305.16930

- **Full Run-2 analysis performed using 139 fb^{-1}**
  - at least 2 jets with p_T > 60 GeV, $|y^{jet}|$< 4.4
  - $H_{T2} = p_{T1} + p_{T2}$ > 400 GeV
  - Measurement performed in inclusive bins of: $N_{jet} \geq 2$, $N_{jet} \geq 5$, H_{T2} > 500, 1000 and 1500 GeV

Generator	Matrix element	PDF set	Parton shower	Hadronisation
PYTHIA	LO	NNPDF2.3 LO	p_T-ordered	Lund String
SHERPA (2 variants)	LO	CT14 NNLO	CS dipole	Cluster || Lund string
POWHEG + PYTHIA	NLO	NNPDF3.0 NLO	p_T-ordered	Lund String
POWHEG + HERWIG	NLO	NNPDF3.0 NLO	Angle-ordered	Cluster
HERWIG (2 variants)	NLO	MMHT2014 NLO	Angle-ordered || Dipole	Cluster

- **The main experimental uncertainties are:**
  - **MC modelling:** from the choice of MC to perform the unfolding. HERWIG angle-ordered vs PYTHIA.
  - **Jet energy scale and resolution:** the resolution dominates in almost all cases

Event isotropies using optimal transport: $1 - I^{128}_{\text{Ring}}$ observable

arXiv.2305.16930

$$1 - I^{128}_{\text{Ring}} = 0.92$$

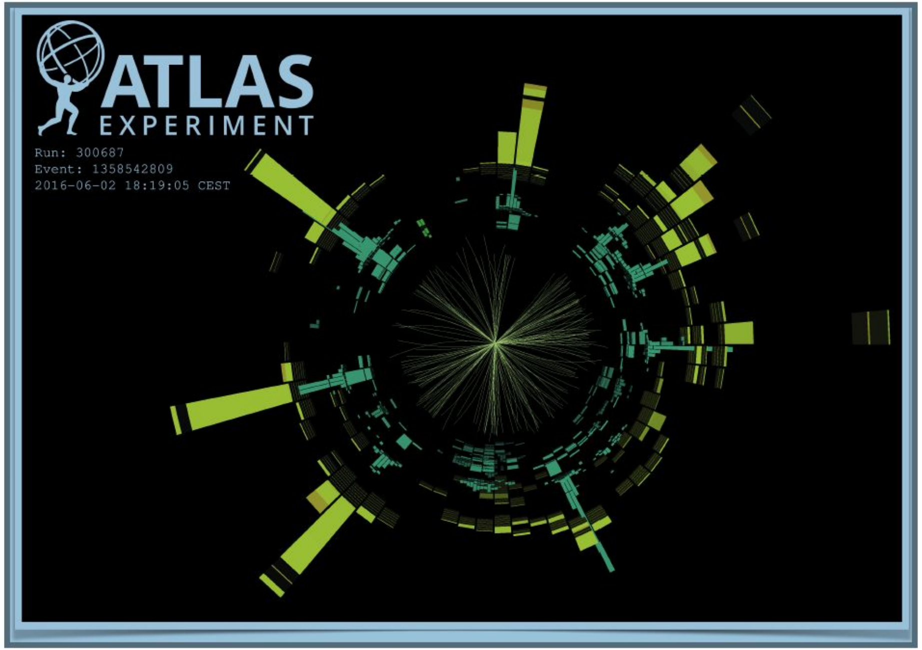

Back-to-back ⟷ Isotropic

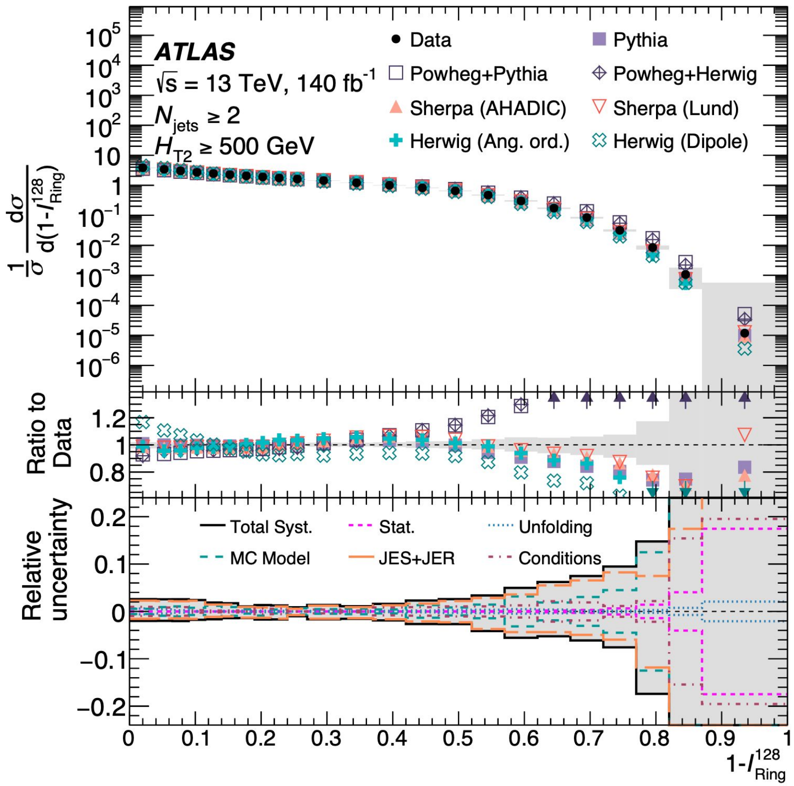

Event isotropies using optimal transport: $1 - I^{128}_{\text{Ring}}$ observable

arXiv.2305.16930

- **Ring-like event isotropy:**
- Measurement of $1 - I^{128}_{\text{Ring}}$ for $N_{\text{jet}} \geq 2$ and $H_{T2} > 500$ GeV
- Distribution is saturated by well-balanced dijets events and by multijet events with isotropic configurations
- Large dynamic range, as the cross section spans by ~6 orders of magnitude
- POWHEG predictions completely disagree with others
- Large differences between HERWIG dipole vs angle-ordered
- No notable differences between SHERPA hadronisation models

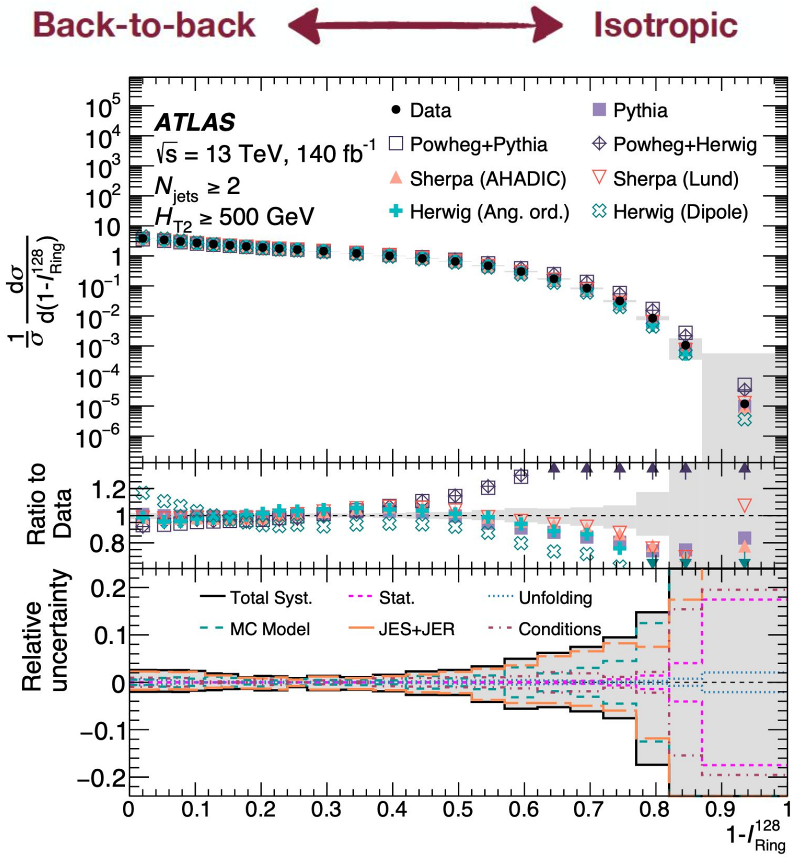

Event isotropies using optimal transport: $1 - I^{16}_{Cyl}$ observable

arXiv.2305.16930

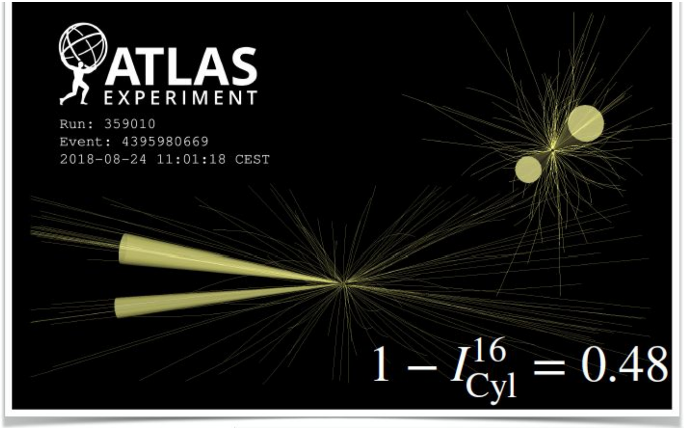

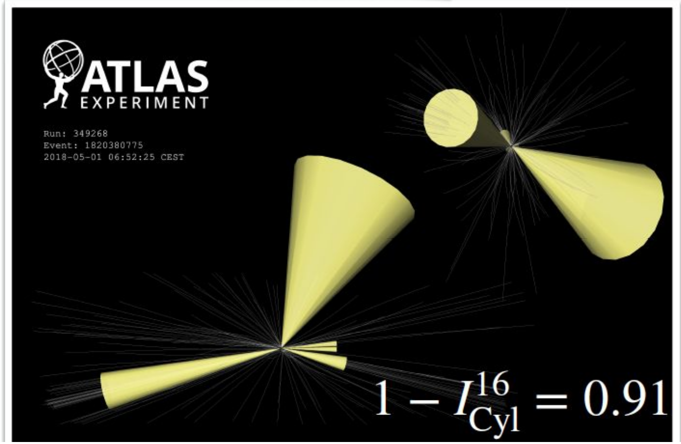

Non-isotropic ⟷ Isotropic

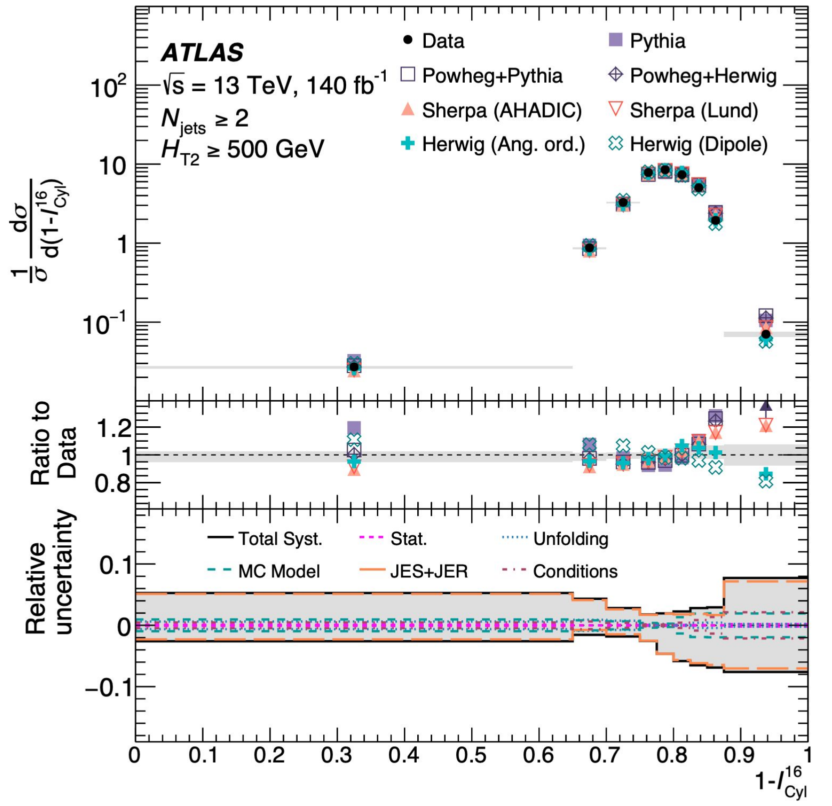

Event isotropies using optimal transport: $1 - I^{16}_{Cyl}$ observable

arXiv.2305.16930

- **Cylindrical event isotropy:**
- Measurement of $1 - I^{16}_{Cyl}$ for $N_{jet} \geq 2$ and $H_{T2} > 500$ GeV
- Distribution is saturated by dijet events in the forward region of one side of the detector and by multijet events that evenly populate the rapidity-azimuth plane
- None of the MC predictions accurately describe this observable
- Different behaviour for different HERWIG parton shower models, PYTHIA and SHERPA predictions
- PYTHIA and SHERPA differ in the tails
- No sensitivity to hadronisation models

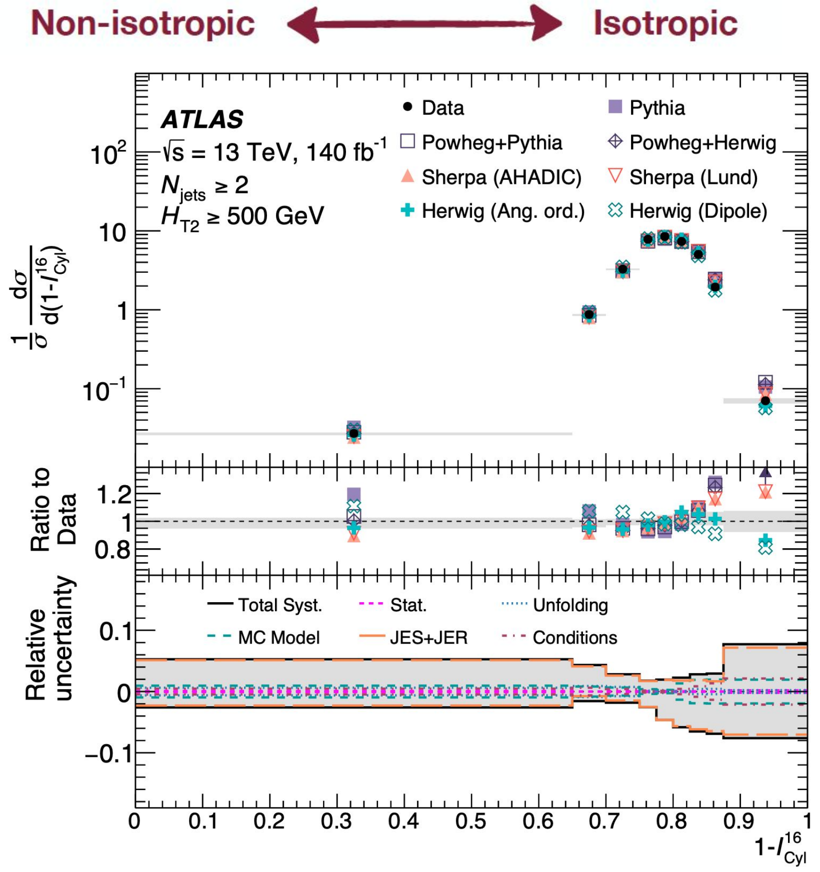

Summay

- **Three ATLAS measurements at 13 TeV using 139 fb^{-1} have been presented**

- **Inclusive-photon production and its dependence on photon isolation:**
  - The dependence on R of the measured cross sections, measured for first time, is well described by NLO JETPHOX and NNLO NNLOJET pQCD predictions
  - Validation of the underlying pQCD theoretical description up to $\mathcal{O}(\alpha_S^2)$

- **Determination of the strong coupling constant from TEEC**
  - Theoretical uncertainties reduced by a factor of 3 thanks to the inclusion of NNLO corrections
  - The evolved $\alpha_S(Q)$ values are compared with the NNLO solution of the RGE showing good agreement up to the highest energy scales and with previous measurements

- **Multi-jet event isotropies using optimal transport:**
  - First application of optimal transport techniques in a collider physics measurement
  - Agreement between unfolded data and simulations tends to be best in balanced dijet-like arrangements and deteriorates in more isotropic configurations

Thanks

IFIC
INSTITUT DE FÍSICA CORPUSCULAR

The ATLAS detector